Inhibition of a spliceosome turnover pathway suppresses splicing defects

Shatakshi Pandit*, Bert Lynn†, and Brian C. Rymond*‡

Departments of *Biology and †Chemistry, University of Kentucky, Lexington, KY 40506-0225

Edited by Michael Rosbash, Brandeis University, Waltham, MA, and approved July 19, 2006 (received for review April 19, 2006)

Defects in assembly are suggested to signal the dissociation of faulty splicing complexes. A yeast genetic screen was performed to identify components of the putative discard pathway. Weak mutant alleles of *SPP382* (also called *NTR1*) were found to suppress defects in two proteins required for spliceosome activation, Prp38p and Prp8p. Spp382p is shown necessary for cellular splicing, with premRNA and, for some alleles, excised intron, accumulating after inactivation. Like *spp382-1*, a mutant allele of *AAR2* was identified in this suppressor screen. Like Spp382p, Aar2p has a reported role in spliceosome recycling and is found with Spp382p in a complex recovered with a mutant version of the spliceosomal core protein Prp8p. Possible insight into to the *spp382* suppressor phenotype is provided by the observation that defective splicing complexes lacking the 5′ exon cleavage intermediate are recovered by a tandem affinity purification-tagged Spp382 derivative. Stringent proteomic and two-hybrid analyses show that Spp382p also interacts with Cwc23p, a DNA J-like protein present in the spliceosome and copurified with the Prp43p DExD/H-box ATPase. Spp382p binds Prp43p and Prp43p requires Spp382p for intron release from the spliceosome. Consistent with a related function in the removal of defective complexes, three *prp43* mutants are also shown to suppress splicing defects, with efficiencies inversely proportionate to the measured ATPase activities. These and related genetic data support the existence of a Spp382p-dependent turnover pathway acting on defective spliceosomes.

pre-mRNA | RNA processing | *spp382* | small nuclear ribonucleoprotein | *Prp43*

Spliceosome assembly in *Saccharomyces cerevisiae* (yeast) extract progresses through the sequential addition of the U1, U2, and U4/U6.U5 small nuclear ribonucleoprotein (snRNP) particles. The snRNP-complete complex then undergoes conformational changes to form a catalytically active enzyme (reviewed in refs. 1 and 2). In this hallmark activation step, the extensively paired U4/U6 snRNAs unwind, and the U6 snRNA displaces U1 at the 5′ splice site and associates with the branchpoint region through U2 snRNA contacts. The U1 and U4 snRNAs dissociate from (or more weakly bind) the mature spliceosome, and neither is required for catalysis. Although alternate models have been proposed e.g., ref. 3, the isolation of cellular U2, U5, and U6 snRNP complexes (4, 5) strongly supports an equivalent spliceosome maturation pathway *in vivo*. This view is reinforced by studies of cotranscriptional premRNA splicing that reveal striking similarities in the timing of splicing factor association *in vivo* and *in vitro* (6, 7).

The specificity determinants for U4/U6.U5 tri-snRNP recruitment to the prespliceosome are unclear, although U5 snRNP-exon interactions and transient U4 and U6 snRNA contacts with the premRNA 5′ splice site region may contribute (1, 8, 9). Once bound, the U5 snRNP-associated Prp28p and Brr2p DExD/H-box proteins are critical for U1 and U4 snRNP release from the spliceosome, respectively (10–13). Other spliceosomal proteins clearly function in this activation step because, for instance, certain mutant alleles of *PRP4*, *PRP38*, and *SNU114* form snRNP-complete, but catalytically impaired, spliceosomes (14–17). Also, reflecting the pivotal role of Prp8p in active site assembly, certain *prp8* mutant alleles suppress growth defects because of *prp28* or *brr2* mutation or resulting from U4/U6 snRNA hyperstabilization (16, 18, 19). Soon after U4 snRNA release, a set of 8–12 proteins, the nineteen complex, tightly binds the spliceosome (20) and stabilizes association of select tri-snRNP recruited factors (4, 21). Subsequently, other DExD/H-box proteins promote conformational changes needed for the first RNA transesterification reaction (Prp2p), the second transesterification reaction (Prp16p, Prp22), mRNA release (Prp22p), and intron release (Prp43p) (1).

Surprising little is known of how spliceosomal DExD/H proteins are recruited, what governs the temporal restriction of activities, or even the principal targets of ATP-dependent function (e.g., RNA unwinding or protein displacement). In contrast, the spliceosome assembly defects associated with the loss of each activity are well established, and, over a decade ago, Burgess and Guthrie proposed a model in which splicing fidelity is coupled to ATP hydrolysis by the Prp16 DExD/H-box protein (22–24). Key to this "kinetic proofreading" mechanism is the existence of a discard pathway to remove defective complexes. Although the components are unknown, such a discard pathway is speculated to act throughout the spliceosome cycle as a quality control system for complex integrity (2).

Here we report the results of a genetic study to identify components of the spliceosome discard pathway. The *prp38-1* mutation causes a temperature sensitive (ts) growth defect because of impaired premRNA splicing (25) that, *in vitro*, results from slow release the U1 and U4 snRNAs (15). We reasoned that the *prp38-1* defect might be relieved by extragenic suppressors that directly enhance splicing efficiency or, alternatively, reduce the turnover of kinetically impaired spliceosomes. Mutant alleles of *SPP382* are shown to suppress both *prp38-1* and *prp8-1* growth defects. Spp382p itself is necessary for splicing and efficient intron metabolism, however, with premRNA and excised intron accumulating after inactivation. Spp382p was previously reported as Ccf8p, a protein implicated in spliceosome dynamics (4) and as Ntr1p, a required factor for Prp43-dependent intron release *in vitro* (26) (henceforth called by its *Saccharomyces* Genome Database standard name, *SPP382*). Consistent with *PRP43* involvement the proposed discard pathway, *prp43* mutants also suppress splicing defects, intriguingly, with efficiencies inversely proportional to the measured ATPase activity. Finally, a mutant in *AAR2* that encodes a spliceosome recycling factor biochemically linked with Spp382p likewise acts as a *prp38-1* suppressor. A possible clue to the *spp382* suppressor activity comes from the observation that, *in vitro*, defective lariat intermediate complexes, lacking the upstream (5′) exon, are specifically recovered with Spp382-Tap. These and related

Conflict of interest statement: No conflicts declared.

This paper was submitted directly (Track II) to the PNAS office.

Abbreviations: BBP, branchpoint binding protein; snRNP, small nuclear ribonucleoprotein; TAP, tandem affinity purification; ts, temperature sensitive.

‡To whom correspondence should be addressed. E-mail: rymond@uky.edu.

 www.pnas.org/cgi/doi/10.1073/pnas.0603188103

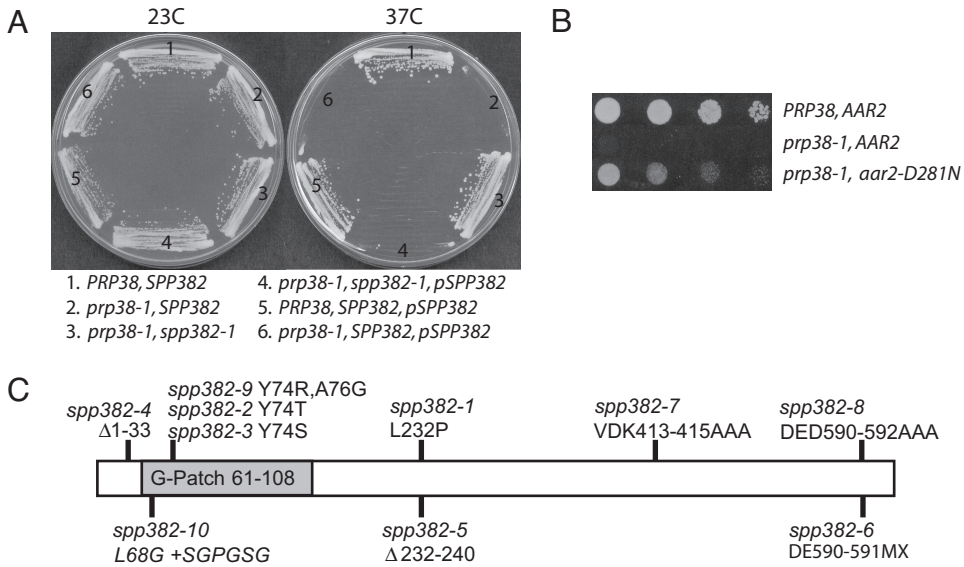

Fig. 1. The recessive *spp382-1* mutation suppresses *prp38-1*. (*A*) Growth of wild-type yeast (streaks 1 and 5), an otherwise isogenic *prp38-1* (ts192) mutant (streaks 2 and 6), and the suppressed mutant (streaks 3 and 4) on rich media after 3 days at the permissive temperature (23°C) or 2 days at the restrictive temperature (37°C). In streaks 4–6, a centromeric yeast plasmid with the wild-type *SPP382* gene (pSPP382) is coexpressed. (*B*) Growth of wild-type yeast (*PRP38* and *AAR2*), the *prp38-1* mutant, and the suppressed *prp38-1, aar2-D281N* double mutant after 2 days at 37°C. (*C*) PCR-based mutagenesis of conserved regions of Spp382p (based on UniProtKB entries: Q06411, Q9UBB9, Q6DI35, Q9NHN7, and Q17784). The amino acid changes and numbered coordinates on the 708-aa protein are indicated above the bar.

studies support a role for the Spp382p–Prp43p intron release complex in the turnover of defective spliceosomes.

Results

Extragenic Suppression of a Spliceosome Activation Mutant. Spontaneous suppressors of the ts *prp38-1* ts mutation were selected on rich medium at 37°C. Two suppressors unlinked to *PRP38* or to the previously identified dosage suppressor, *SPP381* (27), were identified. One results from a D281N substitution in the established splicing factor (28), Aar2p (Fig. 1*B*), whereas the second resided within the then-uncharacterized gene we called *spp382-1*, for the second suppressor of *prp38-1* (Fig. 1*A*). Because *spp382-1* is recessive, the wild-type *SPP382* allele was recovered by screening genomic DNA library transformants for the reacquisition of temperature sensitivity. Linkage analysis shows that orf YLR424W is inseparable from the suppressor locus and thus defines *SPP382*. Plasmid-based *SPP382* expression inhibits growth in the *prp38-1*, *spp382-1* (suppressor) background but does not alter the growth of either wild-type yeast or the ts *prp38-1* mutant in the absence of *spp382-1* (Fig. 1*A*; *pSPP382*).

Suppression by Titration of an Essential Splicing Activity. The 708-aa Spp382p contains a G-patch motif common to a number of RNA binding proteins (reviewed in ref. 30) (Fig. 1*C*). Western analysis identifies Spp382p as Ccf8p, a protein copurified with the Clf1p nineteen complex protein (Ccf8p; S.P., Q. Wang, and B.C.R., unpublished data) (4). Spp382–1p differs from wild type by a L232P substitution downstream of this G-patch. *SPP382* is required for yeast viability (31), but a cellular function in splicing has not been demonstrated. To investigate this possibility, we tested a series of site-directed mutations in regions of high conservation between the yeast, human, zebrafish, fruit fly, and nematode homologs for biological activity.

The plasmid-based mutant alleles were assayed for complementation of a lethal *spp382*::*KAN* disruption after plasmid shuffle to remove a functional *GAL1*::*SPP382* gene. A double G-patch substitution (*spp382-9*) and a more complex G-patch alteration (*spp382-10*) proved lethal (Fig. 1*C* and Table 1), consistent with this being an essential Spp382p motif. Two single amino acid changes within the G-patch (*spp382-2* and *spp382-3*) were viable but showed impaired growth, especially at lower temperatures, whereas a nine-codon deletion within a central domain (*spp382-5*) is tightly ts above 30°C. Two mutants with triple alanine substitutions near the C terminus (i.e., *spp382-7* and *spp382-8*) grow similar to wild type, whereas a nearby frameshift mutation (*spp382-6*) results in slow growth. Finally, an N-terminal deletion that shifts translational initiation to codon 34 (*spp383-4*), supports nearly normal growth when expressed from the *GAL1* promoter.

We next scored the mutant set for *prp38-1* suppression (Table 1). Relative suppressor activity was difficult to quantify because the *spp382* mutations alone cause variable degrees of growth inhibition. Also, we note that *spp382-1*-based suppression is less robust when expressed from the plasmid, possibly because of differences in gene expression. Nevertheless, suppressor alleles were found distributed throughout the coding sequence (i.e., *spp382-1*, *spp382-4*, *spp382-6*, and *spp382-8*), whereas one mutant, the tight ts allele *spp382-5*, was lethal in the *prp38-1* background. None of the mutations suppressed a lethal *prp38*::*KAN* null allele and, similarly, the *prp38-1* mutation did not rescue the lethality of the *spp382-9* or *spp382-10* (data not shown). The simplest interpretation of these observations is that Spp382p is an essential protein which, when limiting, suppresses *prp38-1*.

Spp382p Is Required for Splicing and Normal Intron Metabolism. Whereas incomplete metabolic depletion prevents use of *GAL1*::*SPP382* to assess cellular function (S.P. and B.C.R., unpublished data), transcriptional repression of the functional *GAL1*::*spp382-4* mutant results in time-dependent inhibition of splicing and growth (Fig. 2*A* and data not shown). Primer extension analysis confirms accumulation of *RPS17A* premRNA rather than the similarly sized lariat intermediate (data not shown). No changes are seen with the intronless *ADE3* mRNA, rRNA, or the spliceosomal snRNAs (Fig. 2*A* and data not

BIOCHEMISTRY

Table 1. Growth assays performed in yeast with the indicated *SPP382* allele at 23°C and at 37°C

Allele	23°C	37°C	*prp38-1* suppression
SPP382	+++	+++	NA
prp38-1	++	−	NA
spp382-1	+++	+	Yes
spp382-2	+/−	+	No
spp382-3	+/−	+	No
*spp382-4**	+++	+++	Yes
spp382-5	++	−	Syn. lethal
spp382-6	++	++	Yes
spp382-7	+++	+++	No
spp382-8	+++	+++	Yes
spp382-9	−	−	No
spp382-10	−	−	No

The symbols reflect relative colony sizes from wild-type (+++) to no growth (−). Visible colonies from an otherwise inviable *prp38–1*mutant were indicative of suppression (Yes), whereas no growth indicates lack of suppression (No). NA, not applicable; Syn. lethal, synthetic lethality.

*This allele was expressed with the *GAL1* promoter. All other alleles were expressed with the natural *SPP382* promoter.

shown). For the other site-directed mutants, the level of splicing correlates well with the growth observed (Fig. 2*B* and data not shown). Mutants that support robust growth show little splicing inhibition (e.g., *spp382-7* and *spp382-8*), whereas those with significant growth defects (*spp382-1*, *spp382-2*, *spp382-3*, *spp382-5*, and *spp382-6*) show considerable splicing impairment, typically worse at the elevated temperature. *spp382-7* shows no growth or splicing defects and does not suppress *prp38-1*. Thus, although dispensable for splicing *in vitro* (26), Spp382p is essential for first transesterification step *in vivo*.

Although not apparent with *RPS17A* or *RPL28* probes (Fig. 2 *A–C* and data not shown), splicing is inhibited and excised intron accumulates with several of the *spp382* alleles when *ACT1* is monitored (Fig. 2*B* and data not shown). The relative intron levels do not precisely correlate with apparent splicing inhibition or *prp38-1* suppression, however. Intron accumulation is greatest with central domain mutants (*spp382-1* and *spp382-5*, the latter independent of assay temperature) and with one of the G-patch mutants (*spp382-3*) when assayed at room temperature. Consistent with previous reports (32, 33), this same RNA species accumulates after removal of the Dbr1p 2′–5′ debranching activity or Prp43p (Q. Wang and B.C.R., unpublished data). Finally, we note that splicing enhancement is very subtle in the suppressor strain background when assayed with either *RPS17A* or *RPL28*, indicating that neither ribosomal protein is likely limiting for growth under these conditions (Fig. 2*C* and data not shown).

Spp382p Associates with Defective Spliceosomes. A tandem affinity purification (TAP)-tagged derivative (Spp382-TAP) was used to investigate Spp382p association with *in vitro* assembled splicing complexes. Low levels of both lariat intermediate and excised intron are present Spp382-TAP IgG agarose pellet (Fig. 3*A*). When compared with the input RNA, the recovery of excised intron is favored, especially late in the splicing reaction. Lariat intermediate and excised intron are also recovered, albeit more efficiently, with Prp19-TAP. For both, premRNA, but little or no spliced mRNA, is present in the IgG pellets. As a specificity control, a minor amount of premRNA, but no lariat intermediate or excised intron is recovered with a tagged branchpoint binding protein (BBP-TAP). BBP binds early and transiently to the splicing apparatus, consistent with premRNA signals decreasing to background (WT, no tag) late in the reaction.

Unlike Prp19-TAP, little or no 5′ exon signal is detected in the Spp382-TAP IgG pellet, even with a four-fold increase in exposure time (Fig. 3*A*, compare lanes 16–18 and 28–30). Qualitatively equivalent results were obtained with the *ACT1* premRNA (data not shown). Trace levels of excised intron but no "5′ exonless" intermediates were reported associated with Spp382p in an earlier study (26), although the late-stage reactions used would make such an evaluation problematic. To further investigate this issue, we used an RNA substrate truncated just upstream of the 3′ splice site (Δ3′SS; Fig. 3*B*) for which the lariat intermediate and free exon are terminal products. Nonspecific RNA binding to the resin is negligible (lanes 11 and 12). As with the full-length substrate, lariat intermediate and 5′ exon are recovered from the 30-min splicing reaction with Prp19-TAP in amounts that approximate the 2.5:1 signal ratio expected based on nucleotide content (lanes 9 and 10). With Spp382p, greater levels of lariat intermediate are recovered relative to the full-length RNA, although the relative premRNA recovery did not change. As before, little or no free 5′ exon is found in the IgG pellet (lanes 1 and 2). The trivial possibility that IgG selection causes release of the upstream exon appears unlikely as free (i.e., nonspliceosomal) 5′ exon is resolved by glycerol gradient fractionation before selection (see *Supporting Text* and Fig. 5, which are published as supporting information on the PNAS web site). Here, lariat intermediate molecules are preferentially recovered from lighter, possibly incomplete, spliceosomal fractions. Evidence for spontaneous 5′ exon release from *in vitro* assembled spliceosomes traces back to the origins of this field (e.g., see gradient image in ref. 34). We estimate that under these conditions the 5′ exonless complexes represent

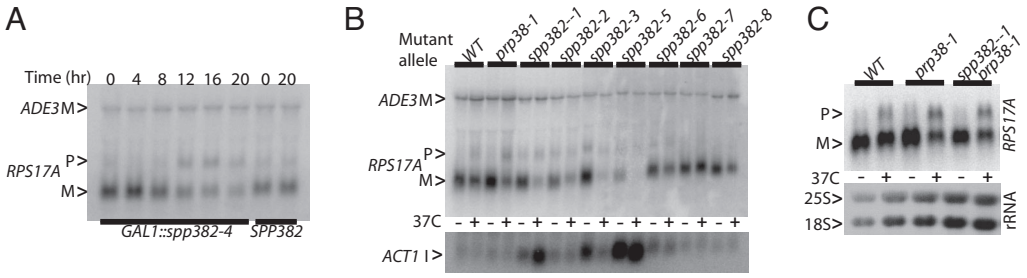

Fig. 2. Loss of Spp382p activity impairs splicing. (*A*) Northern analysis of splicing inhibition in yeast that express the nutritionally regulated *GAL1*::*spp382-4* gene ($T = 0$) and 4–20 h after transcriptional repression by glucose. Wild-type yeast (*SPP382*) were assayed in parallel grown in galactose ($T = 0$) or glucose ($T- = 20$) media. The positions of the intronless *ADE3* mRNA and the *RPS17A* premRNA and mRNA are shown to the left. (*B Upper*) Northern blot analysis as in *A* with wild-type yeast, the *prp38-1* mutant, and the nonlethal *spp382* mutants grown at room temperature (−) or after 2 h at 37°C (+). (*B Lower*) Accumulation of the *ACT1* excised intron RNA. (*C*) Splicing of the *prp38-1* mutant and the *prp38-1*, *spp382-1* double mutant at 23°C and after 2 h at 37°C (+). The 25S and 18S rRNA bands are presented as normalization controls for RNA loading and transfer.

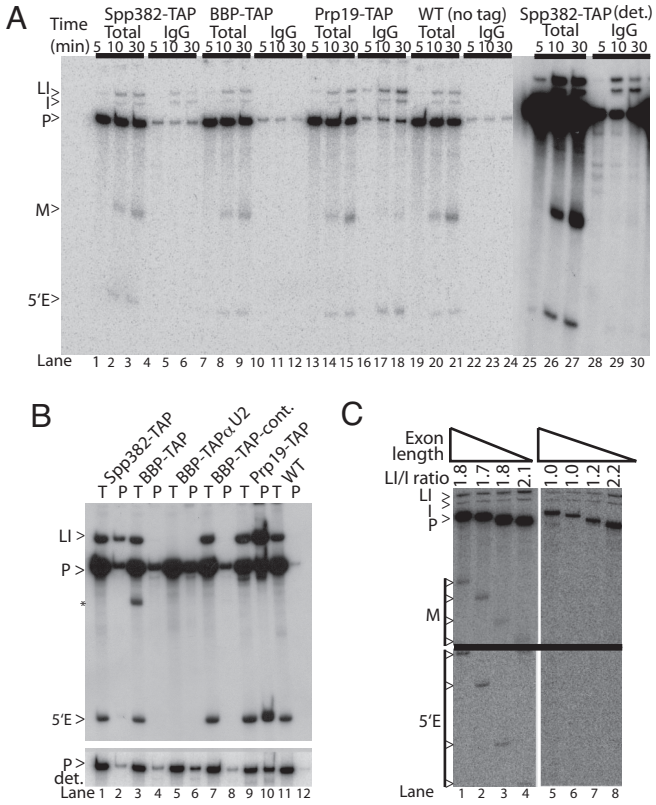

Fig. 3. Spp382p binds defective spliceosomes. (*A*) *In vitro* premRNA splicing with ^{32}P-labeled *RPS17A* premRNA processed for the indicated times under standard conditions and assayed by denaturing PAGE before (Total) or after (IgG) IgG agarose selection. The extracts were prepared from the indicated TAP-tagged strains and from an untagged control (WT). The detail (det.) to the right shows a 4-fold overexposure of the first six lanes to highlight the absence of upstream exon with IgG-agarose selected Spp382-TAP. The positions of the unprocessed premRNA (P), lariat intermediate (LI), excised intron (I), spliced mRNA (M), and free upstream exon (5′E) are indicated. (*B*) *In vitro* splicing and RNA recovery with a 3′ splice site truncated *RPS17A* mRNA. Alternating lanes show the total processed RNA (T) and the IgG agarose pellets (P) after 30 min of splicing. Lanes 5–8 show the results of splicing reactions in which the BBP-TAP extract was preincubated with endogenous RNase H and an oligonucleotide against the U2 snRNA (α U2) or a nonspecific control oligonucleotide (cont.). The asterisk shows the position of linearized lariat intermediate sometimes observed under these conditions. The detail below (det.) shows a 4-fold underexposure of the corresponding premRNA region to highlight the enhanced substrate recovery by IgG agarose after U2 snRNA degradation. (*C*) Extended (+13) or shortened (Δ16, Δ25) 5′ exon *RPS17A* substrates were spliced for 30 min under standard conditions and then assayed for products before (lanes 1–4) or after (lanes 5–8) Spp382-TAP selection. The 5′ exons (below the bar) were run on a second gel to resolve the smaller fragments. In all panels, ≈20-fold more IgG sample is loaded relative to the unfractionated (total) RNA sample. The RNA band intensities were determined with ImageQuant 5.2 (GE Healthcare, Piscataway, NJ).

≈15% of the lariat intermediate pool with this truncated RNA, more than twice that found with the full-length RNA substrate.

Compared with Prp19-TAP, less premRNA is recovered with a BBP-TAP and Spp382-TAP (Fig. 3*B*, compare lanes 2, 4, and 10 with lane 12). Consistent with specific association, however, premRNA recovery is enhanced (and splicing blocked) when the BBP-TAP commitment complex is stabilized by oligonucleotide-directed RNase H digestion of U2 snRNA (compare lanes 4 and 6 in the lower exposure detail). No change is observed when a control oligonucleotide is used (lane 8). In addition, the premRNA recovered with Spp382-TAP exclusively comes from the spliceosomal 40–50S fractions even though most of the premRNA remains in the unassembled pool (see Fig. 5).

Table 2. Spp382p-Cwc23p interactions

Interaction tested	Mass score	Peptides
Spp382-TAP proteins		
Cwc23p	114	3
Rpl14Ap	60	1
Rpl4Ap	27	1
Rep2p	23	1
Rrp5p	20	1
Two-hybrid clone Act:DB*	20 mM 3AT	
SPP382::*Empty*	—	
SPP382::*CWC23*	+++	
CWC23::*SPP382*	+++	
CWC23::*Empty*	—	
WT (*HIS3*) yeast	++++	

Activation domain (Act) and DNA binding (DB) domains.
*Relative colony sizes after 3 days at 30°C.

The data presented above suggests that Spp382p may bind weakly or transiently to a subset of spliceosomal complexes, most surprisingly, defective spliceosomes from which the 5′ exon has been lost. To investigate the role of the upstream exon in sample recovery, we repeated the splicing reactions with *RPS17A* substrates where the 38 nucleotide 5′ exon was lengthened (+13) or shortened by 16 or 25 nucleotides (Fig. 3*C*). As measured by phosphoimaging, the lariat intermediate to fully excised intron (L/I) ratio, an inverse measure of step two splicing efficiency, increases ≈1.2-fold between the shortest and longest substrates (lanes 1–4). In contrast, this ratio more than doubles in the Spp382-TAP-selected pool (lanes 5–8). This greater than proportionate increase reinforces the belief that a distinct subset of lariat intermediates, specifically the defective complexes, are being selected by Spp382-TAP. The number of complexes from which the 5′ exon is lost might increase through stochastic dissociation when the second step of splicing is eliminated (by removal of the downstream exon) or in response to a suboptimal exon sequence (i.e., the truncated 5′ exon). Although the biological relevance of such defective complexes is yet to be established, evidence from Hillern and Parker (35) suggests that splicing complexes containing the lariat intermediate are targets for turnover *in vivo*.

Spp382p Interactions with the Cwc23p J-Domain Protein and the Prp43p ATPase. At low salt concentrations, Spp382p is found in the penta-snRNP (3), the U2, U5, U6 spliceosomal complex (4), and other assemblages of splicing factors, often including Prp43p (36–38). As the complexity of these structures limits inference about primary associations, we repurified Spp382-TAP at high stringency (i.e., 450 mM of NaCl) and assayed for protein association by mass spectroscopy. A single splicing-relevant protein, Cwc23p, was found with high confidence (Table 2). Although the two ribosomal proteins and the 2-μm circle-associated Rep2p present are likely contaminants, the Cwc23p-Spp382p association has been confirmed as a reciprocal two-hybrid interaction (Table 2; and see Fig. 6, which is published as supporting information on the PNAS web site).

Cwc23p was previously recovered with Prp43p (37), a protein that both binds Spp382p and is dependent on Spp382p for intron release *in vitro* (26). In further support of a Spp382p-Prp43p connection, we find that the *prp43R424A* mutation (39) is synthetically lethal with *spp382-4* and *spp382-6* alleles (data not shown). These observations raise the interesting possibility that the suppression of splicing defects by *spp382* mutants occurs through impairment of Prp43p function. For such a suppression mechanism to work, however, Prp38–1p defective spliceosomes must retain partial activity at the restrictive temperature. In agreement, simple overexpression of *prp38-1* with the *GAL1* promoter relieves the ts

BIOCHEMISTRY

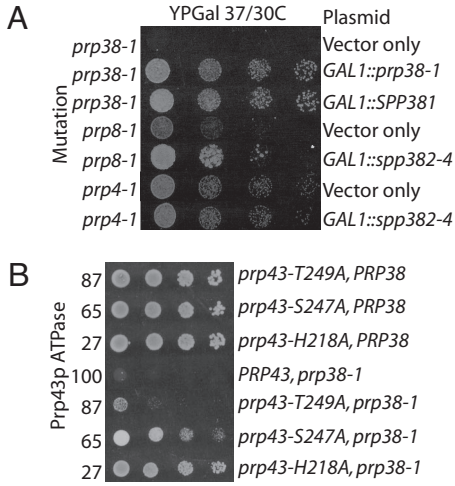

Fig. 4. Genetic characterization of extragenic suppression. (*A*) Yeast with ts *prp38-1*, *prp8-1* or *prp4-1* mutations were transformed with a plasmid to overexpress the *prp38-1* mutant (*GAL1*::*prp38-1*) or the previously characterized *SPP381* dosage suppressor (*GAL1*::*SPP381*). *GAL1*::*spp382-4* was expressed in a *prp38-1*, *SPP382*::*Kan*^{R} background. The cultures were serially diluted and separately plated on yeast extract/peptone/dextrose medium at the restrictive temperature for *prp8-1* (30°C) and *prp38-1* (37°C). To detect even minor changes in growth, a semipermissive temperature of 30°C was used for *prp4-1*. (*B*) Three mutant alleles of *PRP43* assayed for growth at 36°C in the *prp38-1* or wild-type (*PRP38*) background. The Prp43p ATPase activities are from Martin *et al.* (39).

growth defect almost as well as the established *SPP381* dosage suppressor (27) (Fig. 4*A*). Another prediction of this model is that *spp382*-based suppression should not be restricted to *PRP38* mutations. Indeed, we find that the ts *prp8-1* mutant is also suppressed by the *spp382-1*, *GAL1*::*spp382-4*, and *spp382-6* suppressor alleles, although no suppression is observed with a second, arbitrarily selected splicing mutant, *prp4-1* (Fig. 4*B* and data not shown).

To further probe Prp43p involvement, we assayed three viable *prp43* mutants with successively lower ATPase activities for suppression of *prp38-1*. As predicted by the model of Prp43p-remodeling, each *prp43* mutant suppresses *prp38-1* and, remarkably, the degree of suppression is inversely related to the reported ATPase activity (39). And whereas diminished Prp43p activity suppresses *prp38-1*, overexpression of several other yeast genes, including *PRP43*, *CWC23*, and the YNL224C-encoded protein previously purified with Prp43p (37) (that we call *SQS1* for squelch of splicing suppression) impairs *spp382-1*-based suppression (data not shown). Although several explanations for this phenotype are conceivable, the gene-dosage effect is consistent with compensation for reduced Spp382–1p activity by enhanced levels of its associated factors.

Discussion

Under normal circumstances, conformational changes coincident with mRNA formation stimulate Spp382p-dependent Prp43p recruitment or activation resulting in intron release and spliceosome dissociation *in vitro* (26). In support of a similar cellular role, we find that, analogous to *prp43* mutants, certain mutant alleles of *spp382* accumulate excised intron. These alleles include a G-patch mutation within the N-terminal domain that mediates a Prp43p-Spp382p two-hybrid interaction (26, 40, 41) and copurification (38). Although alternative models are conceivable for how reduced *spp382* activity might suppress splicing defects, we favor one based on this established function of Spp382p in complex dissociation. We propose that defects in the splicing complex assembly, for instance because of *prp38-1* or *prp8-1*, promote Spp382p-dependent dissociation of the defective spliceosome through Prp43p. Bolstering this model, we find that *spp382* and *prp43* mutants are synthetically lethal and that Prp43p overexpression is sufficient to impair *spp382-1*-based suppression of *prp38-1*. Finally, and most importantly, we find that *PRP43* mutations with reduced ATPase activity also suppress splicing defects.

In addition to *spp382-1*, *aar2G841A* was found as a spontaneous suppressor of *prp38-1*. Aar2p, together with Prp8p, Snu114p, and the core SM proteins, comprise the16S U5 snRNP particle that copurifies with U1 snRNP and is postulated to act in 5′ splice site recognition (see ref. 28 and references within). The Beggs laboratory (42) recently identified both Aar2p and Spp382p complexed with a mutant version of Prp8p, a protein that binds the 5′ exon before lariat formation (43, 44) and likely assists in its retention afterward (see ref. 45). The defective lariat intermediate recovered with Spp382-TAP might result from modest TAP-based interference with 5′ exon retention or enhanced Spp382-TAP association with (or epitope accessibility within) a defective spliceosome. Notably, Aar2p, like Prp43p and Spp382p, all serve to recycle splicing factors *in vitro* (26, 28, 32). Spliceosomes must function through multiple rounds of catalysis and it is therefore not surprising that the sequestration of limiting proteins in postcatalytic or dead-end splicing complexes should have dire consequences. Recycling factors may act in kinetic competition with factors that promote the completion of splicing or be regulated through specific recruitment or activation steps.

The model presented above is supported by the recovery of both properly excised intron and defective lariat intermediate with Spp382-TAP. Also, the sedimentation profile of the released intron complex (39) is comparable with the nineteen complex fractions enriched with Spp382p/Ccf8p (4), consistent with at least transient association with late splicing complexes. Indeed, given its size and function in intron release, Spp382p is a prime candidate for the unidentified 80-kDa protein that crosslinks to the branchpoint on completion of splicing (47). Our two-hybrid and mass spectroscopy analyses do indicate that Spp382p is tightly associated with the spliceosomal DNA J-domain protein, Cwc23p. Given the role of DnaJ(Hsp40)-like proteins in substrate presentation and Hsp70 ATPase activation (48), Cwc23p association is particularly interesting. Should Cwc23p act similarly in spliceosome turnover, possible ATPase partners include Prp43p and two Hsp70 proteins, Ssa2 and Ssa4, implicated in snRNP dynamics (49) and recovered with the spliceosome (ref. 4). At this point, however, it remains unknown whether all Spp382p-bearing complexes possess Cwc23p or, more generally, how the discard pathway discriminates between defective complexes and authentic spliceosome assembly intermediates.

The spliceosomal DExD/H-box ATPases drive the spliceosome cycle forward and assures fidelity in splicing when coupled with a discard pathway for the removal of flawed complexes (1, 2, 50). The results presented here provide strong evidence for a Spp382p-dependent activity acting on impaired spliceosomes, most likely through Prp43p-stimulated dissociation or reorganization. Although candidates for other pathway components are suggested by this study (i.e., Aar2p, Cwc23p, and Sqs1p), it remains to be learned whether Prp43p function in ribosome biogenesis (38, 46), the turnover of postcatalytic spliceosomes, and the spliceosome integrity activity defined by splicing mutant suppression are accomplished by complexes of equivalent or distinct protein compositions.

Materials and Methods

Yeast Genetics and Plasmid Construction. Spontaneous suppressors of the *prp38-1* mutant, ts192 (25) (α *prp38-1*, *ura3-52*, *trp1-289*, *leu2-112*, *113*, and *his3*), were selected by growth at 37°C on rich medium (yeast extract/peptone/dextrose) (51). Colonies were backcrossed to the wild-type strain, MGD353–13D (*a*, *trp1-289*, *ura3-53*, *leu2-3*,*112*, *arg4*, and *ade2*), sporulated, and the resultant offspring scored for the reappearance of temperature sensitivity

expected for extragenic suppressors. To test for dominance, candidates were mated to the *prp38-1* haploid SP101 (*a*, *prp38-1*, *ura3-52*, *trp1-289*, *leu2-112*, *113*, *his3*, and *arg4*) and the diploid assayed for growth at 37°C. The wild-type *SPP382* allele was identified by transforming SP301 (α *prp38-1*, *spp382-1 ura3-52*, *trp1-289*, *leu2-112*, *113*, and *his3*) with a centromeric yeast DNA library (52) and screening replica plates of the transformants for temperature sensitivity. A PCR approach was used to subclone *SPP382* into vector YCplac33 (53) (primer sequences available on request). Linkage analysis was completed by targeting a *URA3*-linked copy of *SPP382* on plasmid YIpLac211 (53) cleaved with HpaI to its homologous chromosomal locus in strain SPM301. After conformation by Southern blot, the integrant was crossed to wild-type yeast, and the meiotic progeny from 21 tetrads scored for temperature sensitivity.

Inverse PCR with mutagenic oligonucleotides (sequences available on request) and the Expand Long polymerase (Roche Applied Science, Indianapolis, IN) was performed on a YCPlac111 (53) subclone containing the entire *SPP382* orf plus 450 bp of 5′ flanking sequence. The *GAL1*-derivatives were made similarly with pBM150 (for *GAL1*::*SPP382*) (54) and p416 (for *GAL1*::*spp382-4*) (55) and expressed in a *KAN*::*spp382* background of BY4742 (obtained from Open Biosystems, Huntsville, AL). All genes were sequenced before use. Yeast cotransformed a YCp111-*spp382* mutant allele were assayed after *GAL1*::*SPP382* removal by FOA selection (56). Suppression of *prp8-1* was scored by first mating strain SP302 (*a*, *ura3Δ0*, *trp1-289*, *leu2 Δ0*, *his3 Δ1*, *spp382*::*KAN*, and *YCpLac111-spp382-1*), SP102 (*a*, *ura3Δ0*, *trp1-289*, *leu2 Δ0*, *his3 Δ1*, *spp382*::*KAN*, and *p416-GAL1*::*spp382-4*) or strain SP103 (*a*, *ura3Δ0*, *trp1-289*, *leu2 Δ0*, *his3 Δ1*, *spp382*::*KAN*, and *YCpLac111-spp382-6*) with JM640 (*a*, *ade1-1*, *ade2-1*, *ura1*, *tyr1-1*, *his7*, *lys2-1*, *gal1*, and *prp8-1*). Suppression of *prp4-1* was performed similarly. Double mutant haploid isolates were recovered after sporulation and scored for growth on galactose medium at 23°C, 30°C, 33°C, 35°C, and 37°C. Dosage suppression was performed in strain SPM301 after transformation with a plasmid containing the indicated *GAL1*-fusion construct (57). The *PRP43*-based suppression and synthetic lethality assays were done after crossing the *prp43* mutant (α *ura3-52*, *trp1-63*, *his3 Δ200*, *leu2-1*, *ade2-101*, *ade2-101*, *lys2-801*, *prp43*::*KAN*, *p358-prp43*, and *TRP*) with SP101 or the indicated *spp382* mutants.

RNA and Protein Analysis. RNA was recovered from yeast and assayed by Northern blot from a 1% agarose/formaldehyde gel as described (25, 58). Splicing extracts were prepared under liquid nitrogen in a Spex Certiprep 6850 freezer mill as published (59) with TAP-tagged strains (Open Biosystems). Spp382-TAP was purified by IgG agarose and calmodulin agarose affinity selection using standard procedures (29) with NaCl increased to 450 mM in the binding and wash steps. Two-dimensional liquid chromatography and mass analysis was performed with a Deca mass spectrometer (ThermoElectron, Waltham, MA) as described (4). The mass-intensity lists were screened against the nonredundant National Center for Biotechnology Information protein database with MASCOT software (Matrix Science, Boston, MA) at the default cutoff score of 20. The recovery and analysis of radiolabeled substrate with TAP-tagged proteins was done previously for Clf1-TAP (4).

We thank John Woolford for the yeast *prp4* and *prp8* mutants and Beate Schwer for *prp43* mutant derivatives. Support for this work was provided by National Institutes of Health Grant GM42476 (to B.C.R.), and bioinformatic infrastructure funds were provided by National Science Foundation Infrastructure Award EPS-0132295 (to B.C.R.).

1. Brow DA (2002) *Annu Rev Genet* 36:333–360.
2. Konarska MM, Query CC (2005) *Genes Dev* 19:2255–2260.
3. Stevens SW, Ryan DE, Ge HY, Moore RE, Young MK, Lee TD, Abelson J (2002) *Mol Cell* 9:31–44.
4. Wang Q, Hobbs K, Lynn B, Rymond BC (2003) *J Biol Chem* 278:7875–7883.
5. Ohi MD, Link AJ, Ren L, Jennings JL, McDonald WH, Gould KL (2002) *Mol Cell Biol* 22:2011–2024.
6. Gornemann J, Kotovic KM, Hujer K, Neugebauer KM (2005) *Mol Cell* 19:53–63.
7. Lacadie SA, Rosbash M (2005) *Mol Cell* 19:65–75.
8. Newman AJ, Teigelkamp S, Beggs JD (1995) *RNA* 1:968–980.
9. Johnson TL, Abelson J (2001) *Genes Dev* 15:1957–1970.
10. Kim DH, Rossi JJ (1999) *RNA* 5:959–971.
11. Raghunathan PL, Guthrie C (1998) *Curr Biol* 8:847–855.
12. Chen JY, Stands L, Staley JP, Jackups RR, Jr, Latus LJ, Chang TH (2001) *Mol Cell* 7:227–232.
13. Staley JP, Guthrie C (1999) *Mol Cell* 3:55–64.
14. Ayadi L, Miller M, Banroques J (1997) *RNA* 3:197–209.
15. Xie J, Beickman K, Otte E, Rymond BC (1998) *EMBO J* 17:2938–2946.
16. Kuhn AN, Li Z, Brow DA (1999) *Mol Cell* 3:65–75.
17. Bartels C, Klatt C, Luhrmann R, Fabrizio P (2002) *EMBO Rep* 3:875–880.
18. Kuhn AN, Reichl EM, Brow DA (2002) *Proc Natl Acad Sci USA* 99:9145–9149.
19. Kuhn AN, Brow DA (2000) *Genetics* 155:1667–1682.
20. Chen CH, Yu WC, Tsao TY, Wang LY, Chen HR, Lin JY, Tsai WY, Cheng SC (2002) *Nucleic Acids Res* 30:1029–1037.
21. Chan SP, Kao DI, Tsai WY, Cheng SC (2003) *Science* 302:279–282.
22. Burgess SM, Guthrie C (1993) *Cell* 73:1377–1391.
23. Couto JR, Tamm J, Parker R, Guthrie C (1987) *Genes Dev* 1:445–455.
24. Burgess S, Couto JR, Guthrie C (1990) *Cell* 60:705–717.
25. Blanton S, Srinivasan A, Rymond BC (1992) *Mol Cell Biol* 12:3939–3947.
26. Tsai RT, Fu RH, Yeh FL, Tseng CK, Lin YC, Huang YH, Cheng SC (2005) *Genes Dev* 19:2991–3003.
27. Lybarger S, Beickman K, Brown V, Dembla-Rajpal N, Morey K, Seipelt R, Rymond BC (1999) *Mol Cell Biol* 19:577–584.
28. Gottschalk A, Kastner B, Luhrmann R, Fabrizio P (2001) *RNA* 7:1554–1565.
29. Puig O, Caspary F, Rigaut G, Rutz B, Bouveret E, Bragado-Nilsson E, Wilm M, Seraphin B (2001) *Methods* 24:218–229.
30. Aravind L, Koonin EV (1999) *Trends Biochem Sci* 24:342–344.
31. Giaever G, Chu AM, Ni L, Connelly C, Riles L, Veronneau S, Dow S, Lucau-Danila A, Anderson K, Andre B, *et al.* (2002) *Nature* 418:387–391.
32. Arenas JE, Abelson JN (1997) *Proc Natl Acad Sci USA* 94:11798–11802.
33. Chapman KB, Boeke JD (1991) *Cell* 65:483–492.
34. Brody E, Abelson J (1985) *Science* 228:963–967.
35. Hilleren PJ, Parker R (2003) *Mol Cell* 12:1453–1465.
36. Hazbun TR, Malmstrom L, Anderson S, Graczyk BJ, Fox B, Riffle M, Sundin BA, Aranda JD, McDonald WH, Chiu CH, *et al.* (2003) *Mol Cell* 12:1353–1365.
37. Gavin AC, Bosche M, Krause R, Grandi P, Marzioch M, Bauer A, Schultz J, Rick JM, Michon AM, Cruciat CM, *et al.* (2002) *Nature* 415:141–147.
38. Lebaron S, Froment C, Fromont-Racine M, Rain JC, Monsarrat B, Caizergues-Ferrer M, Henry Y (2005) *Mol Cell Biol* 25:9269–9282.
39. Martin A, Schneider S, Schwer B (2002) *J Biol Chem* 277:17743–17750.
40. Uetz P, Giot L, Cagney G, Mansfield TA, Judson RS, Knight JR, Lockshon D, Narayan V, Srinivasan M, Pochart P, *et al.* (2000) *Nature* 403:623–627.
41. Ito T, Chiba T, Ozawa R, Yoshida M, Hattori M, Sakaki Y (2001) *Proc Natl Acad Sci USA* 98:4569–4574.
42. Boon KL, Norman CM, Grainger RJ, Newman AJ, Beggs JD (2006) *RNA* 12:198–205.
43. Teigelkamp S, Newman AJ, Beggs JD (1995) *EMBO J* 14:2602–2612.
44. Teigelkamp S, Whittaker E, Beggs JD (1995) *Nucleic Acids Res* 23:320–326.
45. Grainger RJ, Beggs JD (2005) *RNA* 11:533–557.
46. Combs DJ, Nagel RJ, Ares M, Jr, Stevens SW (2006) *Mol Cell Biol* 26:523–534.
47. McPheeters DS, Muhlenkamp P (2003) *Mol Cell Biol* 23:4174–4186.
48. Walsh P, Bursac D, Law YC, Cyr D, Lithgow T (2004) *EMBO Rep* 5:567–571.
49. Bracken AP, Bond U (1999) *RNA* 5:1586–1596.
50. Query CC, Konarska MM (2004) *Mol Cell* 14:343–354.
51. Kaiser C, Michaelis S, Mitchell A (1994) *Methods in Yeast Genetics* (Cold Spring Harbor Lab Press, Cold Spring Harbor, NY).
52. Rose MD, Novick P, Thomas JH, Botstein D, Fink GR (1987) *Gene* 60: 237–243.
53. Gietz RD, Sugino A (1988) *Gene* 74:527–534.
54. Johnston M, Davis RW (1984) *Mol Cell Biol* 4:1440–1448.
55. Mumberg D, Muller R, Funk M (1995) *Gene* 156:119–122.
56. Boeke JD, Trueheart J, Natsoulis G, Fink GR (1987) *Methods Enzymol* 154:164–175.
57. Gelperin DM, White MA, Wilkinson ML, Kon Y, Kung LA, Wise KJ, Lopez-Hoyo N, Jiang L, Piccirillo S, Yu H, *et al.* (2005) *Genes Dev* 19:2816–2826.
58. Pikielny CW, Rosbash M (1985) *Cell* 41:119–126.
59. Wang Q, He J, Lynn B, Rymond BC (2005) *Mol Cell Biol* 25:10745–10754.